Cayuela *et al. Biochar* (2024) 6:90
https://doi.org/10.1007/s42773-024-00386-3

Biochar

ORIGINAL RESEARCH Open Access

Key biochar properties linked to denitrification products in a calcareous soil

María L. Cayuela[1*], Oliver Spott[2], María B. Pascual[1], María Sánchez-García[1] and Miguel A. Sánchez-Monedero[1]

Abstract

Meta-analyses show an overall decrease in soil N_2O emissions after biochar (BC) amendment. Nonetheless, N_2O mitigation with BC cannot be extrapolated to every BC-soil combination, inasmuch as an increase in soil N_2O release has been occasionally reported. We hypothesized that BC characteristics are key, and performed two microcosm experiments to advance in the understanding of the properties associated. We first investigated how 22 well-characterized BCs affect N_2O emissions in a calcareous soil under denitrification conditions. Whereas most BCs decreased N_2O emissions, some substantially increased N_2O emissions. In a second experiment, we selected and further characterized eight of the 22 previous BCs. We applied the ^{15}N-gas-flux method to study how these BCs affect denitrification products (N_2O and N_2) in the same soil. Results indicate that the interaction between BC and the denitrification process depends on the temperature of pyrolysis. Whereas BCs produced at 400 °C tended to increase total denitrification (N_2O+N_2) by an average of 28%, BCs produced at 600 °C significantly reduced total denitrification by 53%. Nevertheless, this decline in overall denitrification did not result in a decrease of N_2O emissions, as there was a strong shift in the $N_2O/(N_2+N_2O)$ ratio favoring N_2O. A redundancy analysis revealed a direct correlation between carboxylic groups on BCs surface and N_2O emissions. This research enhances our understanding of the interaction of BC with denitrification, particularly concerning the relevance of the temperature of pyrolysis, and opens up new paths for investigation, crucial for optimizing the application of BCs in different soil environments.

Highlights

- High concentration of –COO- groups on BCs surface correlated with the highest N_2O emissions.
- Biochars produced at 600 °C decreased total denitrification (N_2O+N_2).
- Biochars with high electrical conductivity and pH increased NO_2^-/NO_3^- ratios.

Keywords Nitrous oxide, ^{15}N gas-flux method, Denitrification, Pyrogenic C

*Correspondence:
María L. Cayuela
mlcayuela@cebas.csic.es
Full list of author information is available at the end of the article

Springer

Graphical Abstract

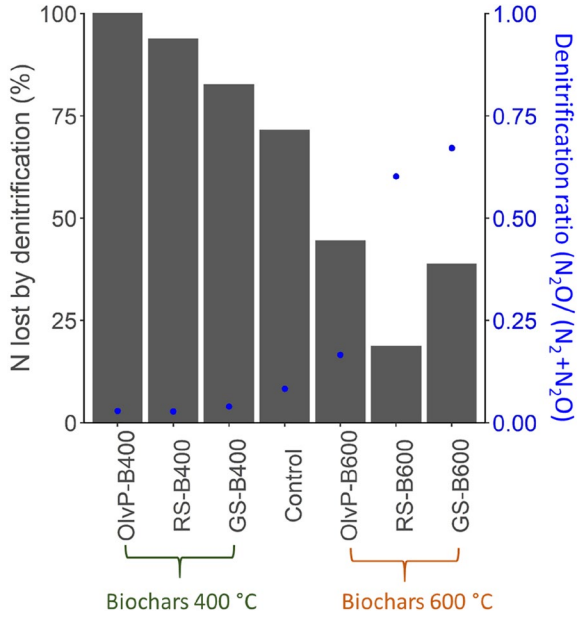

1 Introduction

The concentration of nitrous oxide (N_2O) in the atmosphere has gradually increased at a 2 percent rate over the last century (Tian et al. 2020). It is now clear that nitrogen (N) fertilization to croplands commands this increase, and represents the most important global N_2O source (Winiwarter et al. 2018; Tian et al. 2020). The urgency to mitigate N_2O emissions from agricultural soils has been highlighted in several recent studies (Thompson et al. 2019; Ogle et al. 2020) and potential mitigation strategies are being investigated (Winiwarter et al. 2018; Grados et al. 2022).

One N_2O mitigation strategy that has received growing interest is biochar (BC) soil amendment (Cayuela et al. 2014; Liu et al. 2019; Wu et al. 2023). BC is the solid carbonaceous product from the thermal transformation of organic materials at temperatures between 350 and 750 °C under oxygen-limited conditions (Joseph et al. 2021). BC's most important contribution to climate change mitigation is mostly acknowledged through its potential to sequester organic carbon (C) in soil (Lehmann et al. 2021). However, an additional advantage of BC lies in the lower trade-off between soil C sequestration and N_2O emissions compared to other organic amendments (Cayuela et al. 2010; Maenhout et al. 2024). There is a vast amount of literature that shows a decrease in N_2O emissions after BC soil application, and several meta-analyses demonstrate an overall N_2O mitigation with BC (Kaur et al. 2023). Nonetheless, the high variability of both (i) BC properties and (ii) soil N_2O formation pathways still frustrates any attempts to make confident generalized predictions for specific BC-soil combinations.

A key problem with much of the research on BC and N_2O emissions is the poor characterization of the BCs used in the experiments. Fundamental characteristics such as BC particle size, surface area, H:Corg ratio or, pH are often unaccounted for, e.g. in the database of a recent meta-analysis on N_2O mitigation with BC (Borchard et al. 2019), more than 80% of the studies did not report data on BC atomic H:Corg ratios, which define BC degree of polymerization and stability and are known to influence BC mitigation potential (Cayuela et al. 2015; Weldon et al. 2019). Similarly, very important characteristics known to directly influence soil N dynamics, such as dissolved organic C (DOC), are systematically omitted in BC characterization. DOC is a key parameter, since it can lead to N immobilization in soil, but also stimulate total denitrification and/or decrease N_2O/N_2 ratios (Senbayram et al. 2012). Recent evidence also suggests that other BC properties that are seldom included in the literature (oxygenated functional groups in BC surface, the presence of organic contaminants) might play a relevant role in N_2O emissions (Quin et al. 2015; Yuan et al. 2019).

A second drawback in earlier research on this topic is that studies have mostly focused on total N_2O

emissions, and only a limited number of experiments have explicitly differentiated between N_2O formation pathways (Sanchez-Garcia et al. 2014; Weldon et al. 2019; Dong et al. 2020; Fan et al. 2020). This limits our understanding of the mechanisms of interaction between BC and soil N dynamics and our capacity to establish pilot implementation strategies. As pointed out by Zhu-Barker and Steenwerth (2018), the effectiveness of any N_2O mitigation option is intrinsically linked to the prevailing N_2O formation pathway. In this study, we focused on denitrification, which is, to date, the most studied N_2O formation/consumption pathway with BC. That BC facilitates the last step of denitrification, the transformation of N_2O to N_2, is now widely acknowledged. This facilitation has been linked to a combination of factors: the rise of soil pH in acidic soils (Obia et al. 2015), which might be also related to the increase in the relative gene and transcript copy numbers of the *nosZ*-encoded bacterial N_2O reductase (Harter et al. 2014) as well as direct redox facilitation (Quin et al. 2015; Pascual et al. 2020). However, the effect of BC on total denitrification (N_2O+N_2) is less clear and it is probably very dependent on initial soil and BC properties.

In a series of incubation experiments, Thomazini et al. (2015) applied the same BC to ten different soils under denitrification conditions. They provided evidence that the mitigation potential of BC was positively correlated with the soil N_2O emission rates. They suggested that the inconsistencies across existing BC studies mostly result from variability in BC properties, but that if one specific BC can decrease N_2O emissions in one soil, its effect in other soils could be predicted. The question that remains is: which BC properties are relevant to decrease N_2O emissions or vice versa promote soil N_2O release? and what is the mechanism behind that reaction? That BCs with high N content may increase N_2O emissions is evident, since they supply reactive N to soil microorganisms, fueling nitrification and denitrification processes. That high pH BCs may decrease N_2O emissions in acidic soils is also manifested, since an increase of soil pH is known to favor the transformation of N_2O to N_2, decreasing N_2O emissions. However, to date, not many studies have systematically evaluated how BC properties modulate N_2O/N_2 ratios and total denitrified N. In their seminal study, Weldon et al. (2019) demonstrated a link between BC properties and denitrification product ratios in two acidic soils. Although limited to one feedstock (corncob), pyrolyzed at four highest treatment temperatures (HTT), the study showed the relevance of BC polymerization degree (as defined by H:Corg ratio), BC surface area, and pH as important factors in defining the ability of BC to decrease denitrification N_2O.

The present study builds on the current understanding on this topic through the analysis of the denitrification products (N_2O, N_2) in an agricultural soil with and without BC amendment. The main objective was to understand which BC characteristics are most relevant for soil N_2O mitigation (further than pH and total N concentration) and/or which properties could lead to an increase in N_2O emissions by denitrification. We minimised the pH effect by selecting a soil with a high concentration of $CaCO_3$ and a strong buffer capacity. Considering previous work on the topic, we hypothesized that BC oxygen functional groups, surface area, the presence of toxic compounds such as polycyclic aromatic hydrocarbons (PAHs), and the H:Corg ratios are the most relevant BC properties that ultimately control biochar N_2O mitigation potential.

2 Materials and methods

2.1 Biochars (BCs)

Twenty-two BCs were produced from 11 ligno-cellulosic residues, which were selected based on their prevalence in Mediterranean regions. We included three types of residues: tree pruning (1–5), herbaceous residues (6–9) and residues from relevant agro-industrial activities: wine and olive oil production (10–11). These residues represent a significant opportunity for BC production, as their primary current disposal method is incineration. The selected residues were: (1) almond tree pruning (AP); (2) olive tree pruning (OlvP), (3) orange tree pruning (OP); (4) grapevine pruning (GP); (5) carob tree pruning (CP); (6) giant reed (GR); (7) rice straw (RS); (8) tomato crop (TC); (9) tomato crop with substrate (TC+S); (10) grape stalks (GS) and (11) two-phase olive mill waste (OMW). Residues generated from tomato crops cultivated in soil (TC) consisted of discarded stems, branches, and tomatoes deemed unsuitable for commercialization. Residues from tomato crops grown in greenhouses using peat substrate (TC+S) also included waste from the substrate itself.

Biomass was pyrolyzed at two different highest treatment temperatures (HTT/400 and 600 °C) by slow pyrolysis with a rotatory quartz tube furnace (Nabertherm GmbH. RSR-B 80/500/11. Lilienthal, Germany). The selection of these two HTT was aimed at generating BCs with a diverse range of atomic H:Corg ratios (Table S1), an important characteristic for N_2O mitigation, as indicated by previous studies (Cayuela et al. 2015; Weldon et al. 2019). Before pyrolysis, residues were grinded to a particle size between 1 and 10 mm, ensuring uniformity in the size of the resulting BCs. The residues were first heated to 105 °C under a continuous flow of argon (Ar) (50 L h^{-1}). Subsequently, the temperature increased at a rate of 5 °C min^{-1} until the desired HTT (400 or 600 °C),

which was upheld for two hours (residence time). During HTT, the flow of Ar was increased to 150 L h^{-1}. Finally, the BCs were left to cool down to ambient temperature inside the pyrolyzer, keeping a flux of 50 L h^{-1} Ar. A detailed description of the feedstocks and pyrolysis conditions can be found in Sánchez-García et al. (2019). All BCs were characterized for their physico-chemical properties, including proximate analysis (fixed C, volatile C, and ashes), pH, electric conductivity (EC) and ultimate analysis (C, N, H, O) (ASTM-D1762-84 Chemical Analysis of Wood Charcoal). Oxygen-containing functional groups and N-containing functional groups were determined with X-ray photoelectron spectroscopy (XPS, K-Alpha Xray Thermo Scientific, UK).

A set of eight biochars made from OlvP, RS, TC and GS at 400 and 600 °C were selected and further characterized for physico-chemical properties. The extraction and determination of dissolved organic C (DOC) and total dissolved N (TDN) were performed following the procedure described by Singh et al. (2017). BCs' surface area was determined with mercury intrusion porosimetry (AutoPore V 9600 Micromeritics Instrument, Corp., USA).

The concentration of five of the most abundant PAHs in biochar were also analysed (Hilber et al. 2012). Each BC (in duplicate) was subjected to extraction with toluene (>99.5%, Sigma Aldrich. San Luis, MO, USA) in a rapid automatic soxhlet system (SOXTHERM® C. Gerhardt GmbH & Co. KG, Königswinter, Germany). Two grams of each BC were placed in cellulose thimbles covered with cotton and immersed in 140 mL of toluene containing 4 boiling stones. The extraction temperature was fixed at 208 °C with a reduction interval of 4 min and a reduction pulse of 4 s. A series of extractions, evaporations and rising cycles were set, resulting in an extraction of 12–15 mL in 3 h. This recovered volume was measured precisely and stored in amber glass bottles at 4 °C until analysis. The PAHs determination was carried out in a gas chromatograph–mass spectrometer (GC–MS). The system consisted of an Agilent 7890A (Agilent Technologies, Palo Alto, CA, USA) equipped with an automatic liquid sampler (MPS2) (Gerstel, Mülheim, Germany) and coupled to an Agilent 5975C mass selective detector. The GC was fitted with a diphenyl analytical column Pursuit XRs measuring 100 mm × 3 mm and with a 3 µm particle size (Agilent Technologies, Palo Alto, CA, USA). The starting temperature was set at 100 °C, which was maintained for 1.5 min. Afterwards, a temperature gradient of 10 °C min^{-1} was applied until it increased to 250 °C, where it was maintained for 15 min. Solvent delay was 2.0 min. The injector temperature was 260 °C and its volume of injection was 1 µL. A calibration curve was done with naphthalene, phenanthrene, fluoranthene, anthracene and pyrene standards, using a mixture in toluene of 500 µg mL^{-1} and solid naphthalene at 99% (Sigma Aldrich. San Luis, MO, USA). Two methods were run, the first to scan and the second for quantification, in Selected Ion Monitoring (SIM) (LOD < 5 ppb) adding an internal standard, 1,4-dichlorobenzene-d_4 (98% atom D. Sigma Aldrich. San Luis, MO, USA).

2.2 Soil

The soil, an Haplic Calcisol (WRB 2022), was sampled from the upper layer (0–0.25 m) of a table-grape vineyard in Murcia, Spain (N37°46′44″ O1°33′53.24″). The texture was clay (24% sand, 47% clay and 29% silt) with 59% of carbonates. Soil chemical properties were as follows: 0.71 ± 0.05% organic C (C_{org}), 230 ± 3 mg kg^{-1} dissolved organic C (DOC), 20 ± 2 mg kg^{-1} total dissolved N (TDN), 9 ± 1 mg kg^{-1} NO_3^-–N, <0.1 mg kg^{-1} NO_2^-–N, <0.1 mg kg^{-1} NH_4^+–N, EC of 0.24 ± 0.01 mS cm^{-1} (1:2.5 g water extract), and pH 8.80 ± 0.05 (1:2.5 g water extract). Prior to its use, the soil was air-dried and sieved (<2mm).

2.3 Soil incubation experiments

All incubation experiments were carried out in 250 mL polypropylene jars (Sarstedt. Nümbrecht, Germany), where soil with and without BCs were added. The control (BC0) consisted of 100 g of soil, and the rest of treatments consisted of 98 g of soil and 2 g of the BCs described above (2% w:w). Control soil and soil/BC mixtures were repacked by gently pressing soil with a stainless steel tamper to a soil bulk density of 1.4 g cm^{-3}. All treatments received a solution of KNO_3 (4.4 mmols of N per kg soil, equivalent to 66 mg N kg^{-1} soil for ^{15}N and 62 mg N kg^{-1} soil for unlabelled N), which was added only once at the beginning of the experiment to set the moisture conditions at 90% of the water filled pore space (WFPS), maximizing complete moisture homogeneity. The jars were aerobically incubated at 25 °C (Heraeus, Function Line. Thermo Fisher Scientific, Massachusetts, USA) under darkness, and covered with a wet cotton cloth for minimizing evapotranspiration. Moisture was gravimetrically adjusted in every jar every other day, always after the corresponding gas measurements. The experiments were laid out as a randomized block design with four replicates per treatment.

2.3.1 Experiment 1: Effect of 22 BCs on total N_2O emissions from soil

A first experiment was set up to explore potential relationships between BCs properties and soil N_2O emissions. A total of 92 jars (four replicates of each BC treatment and a control) were incubated during 27 days under the conditions reported above. BCs were ground to a particle size <1 mm before their mixture with soil. Gas

(N_2O, CO_2 and CH_4) fluxes were regularly monitored at days 0, 1, 2, 3, 4, 6, 7, 8, 9, 10, 13, 16, 20 and 27. For N_2O sampling, each unit was sealed with gas-tight polypropylene screw caps for an accumulation period of 60 min. Changes in the concentration of N_2O after closing the caps were determined with a photo-acoustic monitor 1412i gas chromatograph (Lumasense Technologies A/S, Ballerup, Denmark), which was directly attached to the jars by two Teflon tubes and needles through septa. The gas analyzer was fitted with optical filters to selectively measure concentrations of CO_2, N_2O, CH_4 and water vapor. The photoacoustic analyzer was regularly calibrated by the manufacturer for CO_2, N_2O and CH_4 with certified standards and the concentrations of N_2O were automatically compensated for the interference of CO_2 and water vapor. Additionally, calibration curves for CO_2 (up to 1000 ppmv) and N_2O (up to 25 ppmv) were performed to check the linearity of the measurements. We considered the potential interference of CO_2 on N_2O measurements, as outlined by Harvey et al. (2020). Upon verification, we confirmed the absence of interference at CO_2 levels below 1000 ppm. This threshold represented the highest recorded CO_2 concentration in the jars headspace after 1 h of accumulation. N_2O fluxes were calculated assuming a linear increase during the accumulation period, an approach that was verified prior to and during the experiments.

2.3.2 Experiment 2: Effect of eight selected BCs on denitrification products (N_2O and N_2) and mineral N dynamics in soil

Eight BCs, derived from different feedstocks (wood, straw, herbaceous, agro-industrial residues), were selected considering their contrasting physicochemical properties and their influence on soil N_2O emissions in the previous exploratory experiment: OlvP-B400 and OlvP-B600, associated with no change and decreased N_2O emissions respectively; RS-B400 and RS-B600, linked to decreasing and increasing emissions; TC-B400 and TC-B600, both associated with decreased emissions and GS-B400 and GS-B600, linked to no change and increased emissions. This time BCs were added to soil with a particle size between 1 and 10 mm (i.e. they were not grinded after pyrolysis) with the aim of taking into account their physical properties such as bulk density and pore area.

In this experiment the ^{15}N gas flux method was applied to quantify denitrification products (Micucci et al. 2023). Labelled $K^{15}NO_3$ (Potassium Nitrate-^{15}N. 99 atom% ^{15}N. CAMPRO Scientific GmbH, Germany) was added at the same rate as in experiment 1 (4.4 mmols of N per kg of soil) to air dry soil samples with/without BCs. Working with dry soil when applying tracers has been found to improve the uniform distribution of the tracer in soil and therefore minimise the potential underestimation of denitrification (Berendt et al. 2020). Headspace gas samples of 12 mL were withdrawn after an accumulation period of 1 h as in the previous experiment. Gas samples were taken at 0, 24, 48, 96, 144, 168, and 258 h and stored in evacuated 12 mL glass vials (Labco Exetainer®. Lampeter, UK). A total of 252 samples (9 treatments × 4 replicates × 7 sampling times) were analyzed for their isotope ratios of N_2 (29/28 (^{29}R) and 30/28 (^{30}R)) and N_2O (45/44 (^{45}R) and 46/44 (^{46}R)) at the Stable Isotope Facility (University of California, Davis, USA) by automated isotope ratio mass spectroscopy (ThermoFinnigan GasBench & PreCon trace gas concentration system interfaced to a ThermoScientific Delta V Plus isotope-ratio mass spectrometer, Bremen, Germany).

In addition, CO_2 fluxes were regularly monitored at days 0, 1, 2, 3, 4, 5, 6, 7, 8, 9 and 11 with a photo-acoustic monitor 1412i gas chromatograph, as in experiment 1.

A parallel incubation with nine extra replicates of each treatment was set up for destructive soil sampling and analyses of NO_3^- and NO_2^- at 24, 48 and 96 h. Additionally, NH_4^+, $NO_2^-$and NO_3^- were analysed the last day of the incubation (258 h). The extraction of NO_3^-, NO_2^- and NH_4^+ was carried out by shaking 0.8 g of moist soil 1:10 (dw/v) with water (for NO_3^-, NO_2^-) or 2.0 M KCl (for NH_4^+) for 2 h. Afterwards, the extracts were centrifuged (2509×*g*) and filtered (0.45 µm). The quantification of NO_3^- and NO_2^- in the extracts was performed with ion chromatography (HPLC, model 861, Metrohm AG, Herisau, Switzerland). In the case of NH_4^+, a colorimetric method based on Berthelot's reaction was followed (Sommer et al. 1992).

2.3.3 Calculations and statistical analyses

Cumulative N_2O emissions were calculated assuming linear changes in fluxes between adjacent measurement points, according to the standard trapezoidal estimation. In experiment 2, N_2O and N_2 produced by denitrification were calculated based on ^{15}N data using a two-pool model approach reported by Spott et al. (2006), assuming denitrification of a homogenously labelled soil nitrate pool as the only relevant source of $^{15}N_2O$ and $^{15}N_2$ formation with only unlabelled N_2O and N_2 (e.g. fed by atmosphere) as a second contributor (Pool 1). At first, ^{15}N labelling of nitrate (i.e. source of $^{15}N_2O$ and $^{15}N_2$) was calculated for each gas sampling event using the ^{15}N data of sampled N_2O as follows:

$$a_2 = \frac{\alpha_{46} - a_1 \cdot a_m}{a_m - a_1} \quad (1)$$

where a_2 is the ^{15}N mole fraction of labelled nitrate currently denitrified to N_2O, a_1 is the ^{15}N mole fraction of

the unlabelled N gas Pool 1, and a_m is the ^{15}N mole fraction of sampled N_2O. Subsequently, current labelling of the ^{15}N nitrate pool was used to calculate the contribution of denitrified N_2O to the two-pool N_2O gas mixture as follows:

$$d_{N_2O} = \frac{a_m - a_1}{a_2 - a_1} \quad (2)$$

where d_{N2O} represents the relative fraction of denitrified N_2O on the total N_2O gas volume analyzed. In contrast to N_2O, ^{15}N enrichment of sampled N_2 was very low due to an atmospheric N_2 background concentration of 78%. At very low ^{15}N enrichments IRMS systems tend to cause an erroneous determination of mass 30 of N_2 (i.e.$^{15}N^{15}N$) due to interferences with NO gas ($^{14}N^{16}O$) formed during analysis. Therefore, another approach was used for calculating the contribution of denitrified N_2. When denitrified N_2O is assumed to act as a direct precursor to denitrified N_2, ^{15}N abundance of the labelled nitrate pool as calculated by highly enriched N_2O (i.e. a_2) can be assumed to be equal for denitrified N_2. By using a_2 based on denitrified N_2O, the contribution of denitrified N_2 can be calculated independent from mass 30 by using the following equation:

$$d_{N_2} = \frac{1}{1 - \frac{^{29}R(1-a_2)^2 - 2a_2(1-a_2)}{^{29}R(1-a_1)^2 - 2a_1(1-a_1)}} \quad (3)$$

where d_{N2} represents the relative fraction of denitrified N_2 in the total N_2 gas volume and ^{29}R represents the mass ratio of $^{29}N_2$ and $^{28}N_2$ in N_2 gas volume.

Finally, calculated contributions were used to compute N_2O and N_2 fluxes due to denitrification using total gas concentration sampled during 60 min of closing the incubation vessels similar to experiment 1. Extreme outliers in these N_2O and N_2 flux data (<5% of the dataset) were identified and systematically removed considering the median absolute deviation (MAD). In view of the high dispersion of data for gas measurements, we took a very conservative approach and discarded data when the difference with the median was higher than ten times the MAD, i.e. [xi − median (xi)]/MAD > 10), where median (xi) is the median of all the xi values (gas fluxes) and MAD = median [xi − median(xi)] (Miller and Miller 1992).

N_2O and N_2 data were ln-transformed to improve symmetry and homogenize the variance before analysis. The differences between treatments were determined with a one-way analysis of variance (ANOVA) with the use of IBM SPSS Statistics 29. Additionally, to explore the relationship and multivariate correlations between the tested BC's physicochemical properties and soil gas emissions, a redundancy analysis (RDA) was carried out using Canoco 4.5 for windows. BCs characteristics were included as predictor variables. For the first experiment there were 88 observations (22 BCs in quadruplicate), and the dependent (response) variables were cumulative N_2O and CH_4 emissions. For the second experiment, there were 32 observations (8 BCs in quadruplicate) and total cumulative N_2O and N_2 emissions and NO_2^-/NO_3^- ratios were included as the dependent variables. There were 15 explanatory variables (NO_3^-, NO_2^- and NH_4^+ concentrations in BCs were excluded, as they were negligible). To take into account how much of the variance of the canonical coefficients was inflated by the presence of correlations among explanatory variables, the variance inflation factor (VIF) was used to remove variables. VIF measures the instability of the regression model and, as a rule of thumb, variables that have a VIF higher than 20 should be removed from the model. To avoid correlations among explanatory variables, those with the highest variance inflation factor (VIF) were removed from the analysis at a time and the analysis recomputed. This iteration was repeated as many times as necessary until VIF of all selected variables was lower than 20. Significance of the ordination axes was calculated by the Monte-Carlo permutation test with $n = 999$ (Ter Brak and Smilauer 1998). Graphs were drawn with ggplot2 package (Wickham 2016) and CanoDraw 4.5 for RDA ordination plots.

3 Results

3.1 Overview of main BCs properties

The general physico-chemical properties of BCs are summarized in Table S1. All residues selected for the production of BCs were lignocellulosic and as a result all BCs had relatively low concentrations of total N (between 0.6% in RS-B600 and 2.4% in GP-B400). Total organic C (C_{org}) was between 67% and 85% in woody biochars (produced from pruning residues) and remained generally lower in BCs from herbaceous residues and secondary agro-food wastes (41–74%). All BCs were alkaline (pH between 9.3 and 12.3). The EC values were generally low (0.6–4.5 mS cm^{-1}) with the exception of BCs produced from olive mill wastes, rice straw, and particularly tomato crop, whose EC reached 23 mS cm^{-1}. Ash concentrations were also higher in BCs produced from these residues. The EC and ash concentration increased with the HTT of pyrolysis. The $H:C_{org}$ molar ratios were between 0.23 (OlvP-B600) and 0.90 (TC-B400). Both $H:C_{org}$ and $O:C_{org}$ ratios decreased with increasing HTT. All BCs produced at 600 °C had a $H:C_{org}$ below 0.5. Regarding oxygenated functional groups in BCs surface, an increase in HTT from 400 to 600 °C resulted in a decrease of oxygenated species (C–O (hydroxyl, ether), C=O/O–C–O (carbonyl or carbon linked to two ether/hydroxyl bonds) and –COO (carboxyl). However, this was mostly for –C–O and

C=O/O–C–O groups and not evident for –COO, since GS-B600 and OMW-B600 showed the highest relative atomic percentages of carboxylic groups. N-containing functional groups could not be quantified because of the low N concentrations in the BCs, leading to very low N1s signals.

Table S2 shows the additional characterization of the eight selected BCs used in experiment 2. The DOC values were markedly affected by the feedstock. In general, DOC concentrations were low, and remained below 2.8 mg g^{-1} in all BCs, except for TC-B400, GS-B400 and GS-B600, which were 7.5, 8.0 and 6.9 mg g^{-1}, respectively. Total dissolved N (TDN) was very low (<0.4 mg g^{-1}) in all BCs, with concentrations of NO_3^- and NO_2^- below the quantification limits and negligible concentrations of NH_4^+. The highest total pore areas (TporeA) were found in OlvP BCs and the lowest in TC BCs. TporeA generally increased with HTT (except for rice straw BC). The analysis of the PAHs in the BCs showed, in general, low concentrations in the range of ng g^{-1} BC (Table S2). Overall, the most abundant PAH in the BCs was naphthalene, followed by anthracene. The concentrations of phenanthrene and pyrene were close or below the limit of quantification in all BCs. OlvP-B600 and RS-B600 had the greatest concentrations of the measured PAHs, 176.6 and 152.5 ng g^{-1} BC, respectively.

3.2 Experiment 1: Total N_2O emissions from BCs amended soil and their relation with BCs properties

Nitrous oxide fluxes reached the maximum rate within the first ten days of incubation and were not significantly different to zero after 20 days (Figure S1). BC application affected the dynamics of soil N_2O fluxes (Figure S1) and also total cumulative N_2O emissions (Fig. 1). Out of the 22 BCs assessed, eleven exhibited a significant reduction in N_2O emissions ($P < 0.05$), with an average decrease of 48%. Seven BCs showed no statistically significant difference compared to the control, while four BCs demonstrated a significant increase in N_2O emissions, in the order: RS-B600 > OMW-B600 > GR-B400 > GS-B600.

No significant correlations were found between single BC properties (detailed in Table S1) and total cumulative N_2O emissions (see the Pearson correlation matrix in Figure S2). Significant correlations were found between BC

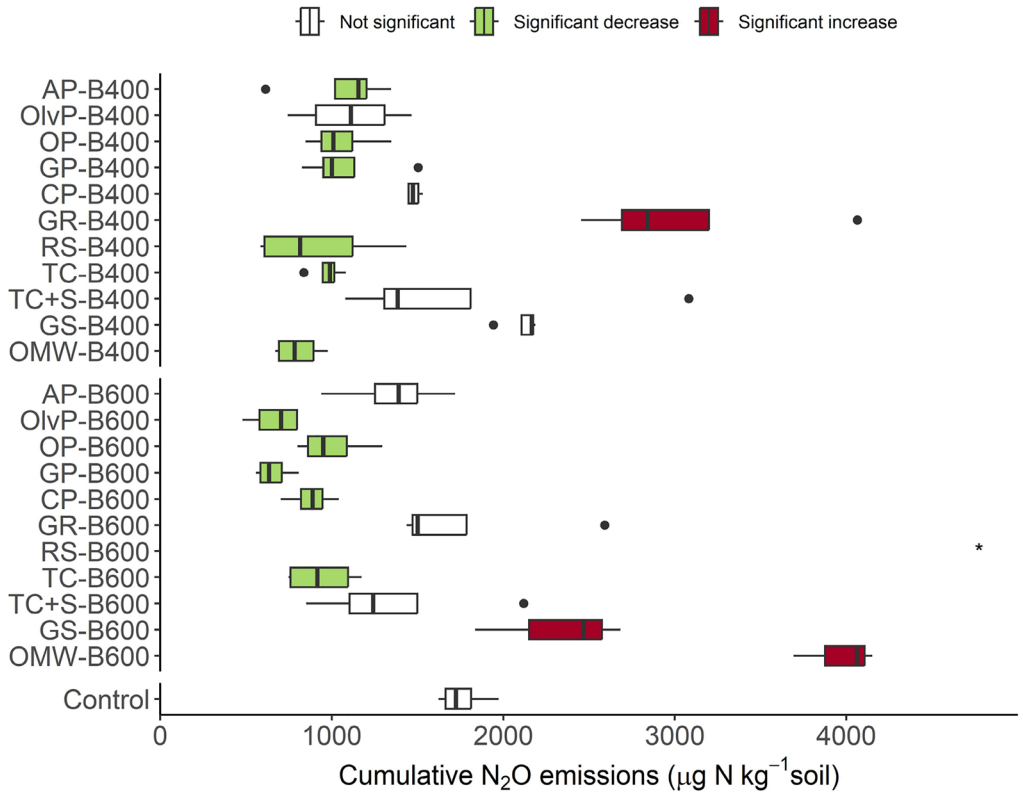

Fig. 1 Boxplots showing total cumulative N_2O emissions after 27 days in control soil and after amendment with 22 biochars applied at a rate of 2% dry weight. *To ensure a representative visualization of the majority of the data points, data for RS-600 (median: 14,631) are shown in Figure S4. Control: soil without biochar, *AP* almond tree pruning, *OlvP* olive tree pruning, *OP* orange tree pruning, *GP* grapevine pruning, *CP* carob tree pruning (CP), *GR* giant reed, *RS* rice straw, *TC* tomato crop, *TC+S* tomato crop with substrate, *GS* grape stalks and *OMW* two-phase olive mill waste. B400 and B600 indicate the highest temperature of pyrolysis: 400 and 600 °C, respectively

properties, e.g. there were direct correlations between (i) total organic C and fixed C, (ii) ash concentration and electrical conductivity and (iii) H:C and O:C ratios in BCs and indirect correlations between (i) ash and total organic C and (ii) C:N ratio and total N. Total cumulative CH_4 emissions are depicted in Figure S3. There was a strong correlation between total cumulative N_2O and CH_4 emissions ($r^2 = 0.939$; $P < 0.001$).

3.3 Experiment 2: Effect of eight selected BCs on denitrification products and mineral N dynamics

3.3.1 Denitrification products (N_2O, N_2) from BCs amended soils

Figure 2 shows total cumulative N_2O (A) and N_2 (B) loss by denitrification at the end of the incubation (≈11 days) for the control soil and the eight selected BCs. In general, BCs produced at 400 °C showed a tendency to decrease N_2O emissions and increase N_2 emissions compared to the control soil, although not statistically significant. On the contrary BCs produced at 600 °C tended to increase N_2O emissions and decrease N_2 emissions. BCs from tomato crop residues were the only exception since TC-B400 increased N_2O emissions, with no significant effect on N_2 emissions, and TC-B600 substantially decreased both N_2O and N_2 emissions.

Table 1 shows the denitrification ratios ($N_2O/(N_2O+N_2)$) and the percentage of N lost by denitrification (N_2O+N_2) with respect to the initially added NO_3^-–N (TC-Bs were excluded as they will be discussed separately). After 258 h, N loss by denitrification in the control soil was 72% of the NO_3^- added, but only 8% of the total loss was as N_2O (i.e. the denitrification ratio was 0.08). Although not statistically significant, the addition of BCs at 400 °C consistently decreased the denitrification ratio to less than half. Additionally, there was a tendency for an increase in the total N turnover by denitrification of added nitrate (between 83% and 100%). In contrast, the addition of BCs produced at 600 °C significantly decreased the total N turnover by denitrification (on average 34% of fertilized nitrate) while simultaneously increased the contribution of N_2O on total N loss (i.e. total denitrification was restrained in favor of a diminished and incomplete denitrification to N_2O). GS-B600 exhibited the highest increase of the denitrification ratio, where N_2O accounted for over half (67%) of the denitrification products.

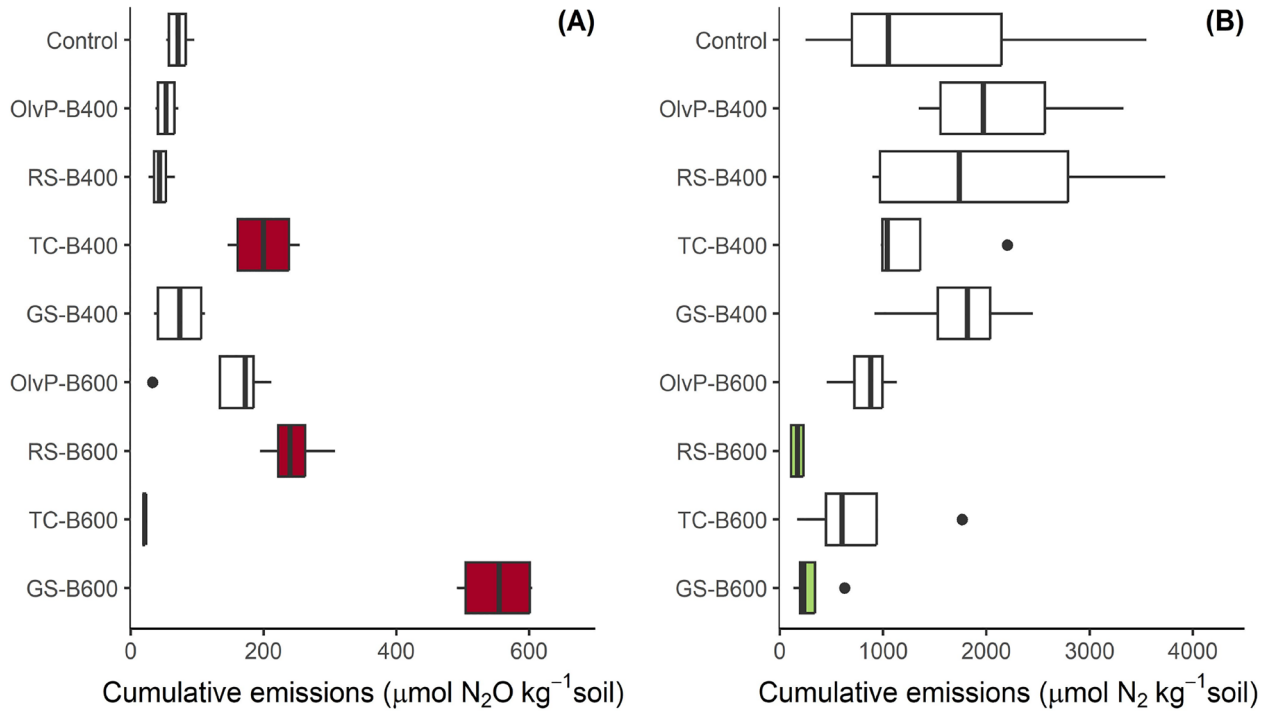

Fig. 2 Boxplots showing total cumulative N_2O (**A**) and N_2 (**B**) emissions (µmol N_2O (or N_2) kg^{-1} soil) after 258 h of incubation. Values are given in µmol instead of µg of N due to the variable ^{15}N signature in gas molecules, which affects the accuracy of reporting mass weight. Different colours indicate significant differences between treatments and control according to the Dunnet test ($P < 0.05$): *green* significant decrease, *red* significant increase. *OlvP* olive tree pruning, *RS* rice straw, *TC* tomato crop, *GS* grape stalks. B400 and B600 indicate the highest temperature of pyrolysis: 400 and 600 °C, respectively

Table 1 Denitrification ratios ($N_2O/(N_2O+N_2)$) and percentage of N lost by denitrification after 258 h (~11 days) of incubation for individual BCs (A) and BCs grouped by temperature of pyrolysis (B)

(A)	Control	OlvP-B400	RS-B400	GS-B400	OlvP-B600	RS-B600	GS-B600
$N_2O/(N_2O+N_2)$	0.083	0.029	0.028	0.040	0.166	0.602	0.671
SE ($n=4$)	(0.022)	(0.009)	(0.008)	(0.007)	(0.053)	(0.042)	(0.066)
Dunnet test		NS	NS	NS	NS	***	***
N loss (%)	72	100	94	83	45	19	39
SE ($n=4$)	(19)	(20)	(31)	(15)	(6)	(2)	(6)
Dunnet test		NS	NS	NS	NS	**	NS
(B)	**Control**		**B400**			**B600**	
$N_2O/(N_2O+N_2)$	0.083		0.032			0.480	
SE ($n=12$)	(0.022)		(0.004)			(0.073)	
Dunnet test			NS			***	
N loss (%)	72		92			34	
SE ($n=12$)	(19)		(12)			(4)	
Dunnet test			NS			*	

Mean values ($n=4$ for individual BCs; $n=12$ for BCs at 400 and 600 °C). Numbers between brackets show standard errors of the mean. The Dunnet post hoc test was used to compare the treatments with the control soil (*NS* not significant, $^*P<0.1$; $^{**}P<0.01$; $^{***}P<0.001$). Control: soil without BC, *OlvP* olive tree pruning, *RS* rice straw, *GS* grape stalks. B400 and B600 indicate the highest temperature of pyrolysis: 400 and 600 °C, respectively

3.3.2 Mineral N dynamics from BCs amended soil

Figure 3 shows the concentration of water-extractable NO_3^- and NO_2^- during the incubation. Nitrate was the most abundant mineral N form and decreased from 39 mg N kg^{-1} soil (24 h) to 3 mg N kg^{-1} soil (258 h) in the control soil. Nitrate concentration was very constant for the first 96 h (Figure S5), which fits well to the observed pool dilution, which was largest within the first 100–150 h, indicating larger NO_3^- production within that time. Most BCs did not modify mineral N dynamics in

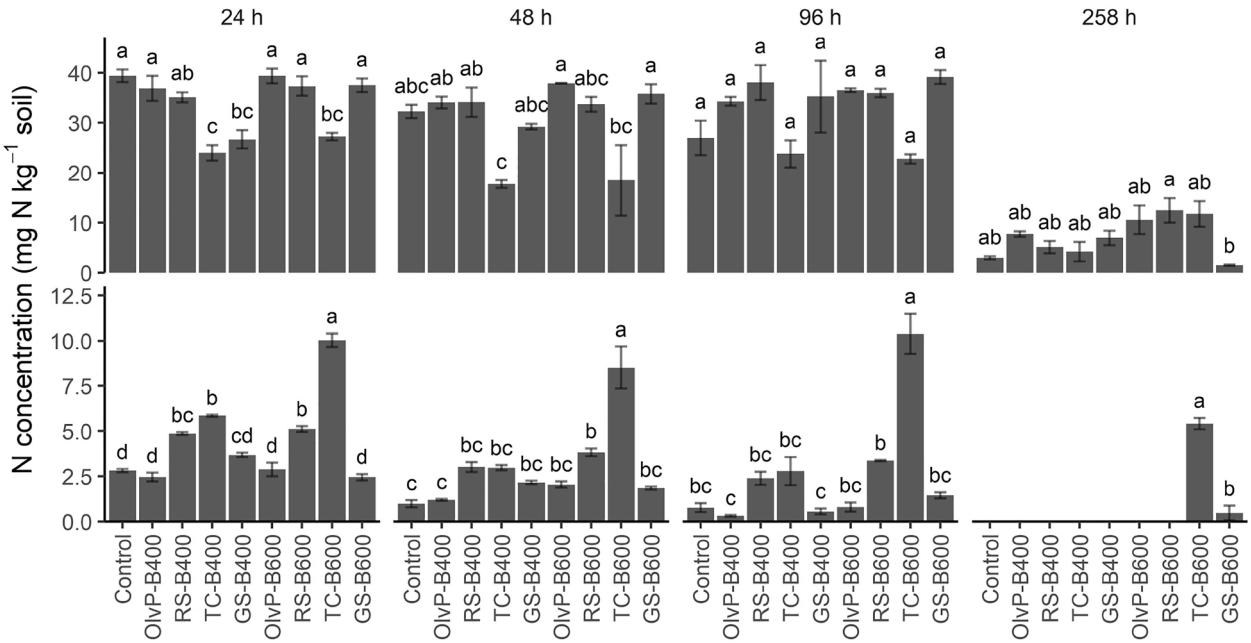

Fig. 3 Water-extractable NO_3^- (top panel) and NO_2^- (bottom panel) concentrations in soil (mg N kg^{-1} soil) for the different treatments after 24, 48, 96 and 258 h. Error bars indicate standard error of the mean ($n=3$). Different letters (a, b, c, d) show significant differences between treatments according to the Tukey test ($P<0.05$) (Figure S5 shows significant differences between sampling times for the same treatment). *OlvP* olive tree pruning, *TC* tomato crop, *RS* rice straw, *GS* grape stalks. B400 and B600 indicate the highest temperature of pyrolysis: 400 and 600 °C, respectively

soil, except for the BCs produced from tomato plants, which showed significantly lower concentrations of NO_3^- than the rest of the treatments at 24 and 48 h. These BCs also showed the highest concentration of NO_2^- in soil throughout the incubation, especially TC-B600. The rest of the treatments showed low NO_2^- concentrations, constantly below 5 mg N kg^{-1} soil.

Ammonium concentrations at the end of the incubation were lower than 8 mg kg^{-1} soil for all treatments (Figure S6). OlvP-B600 and RS-B600 led to significantly lower concentrations of NH_4^+ (4.4 mg N kg^{-1} soil) compared to the control (7.4 mg N kg^{-1} soil).

3.3.3 Relationships between denitrification products and BCs properties

Figure 4 shows the canonical orgination diagram showing the relationship between BCs characteristics and total cumulative N_2O emissions in the first experiment. The diagram delineates three distinct categories of BCs with respect to their impact on N_2O emissions: (i) BCs

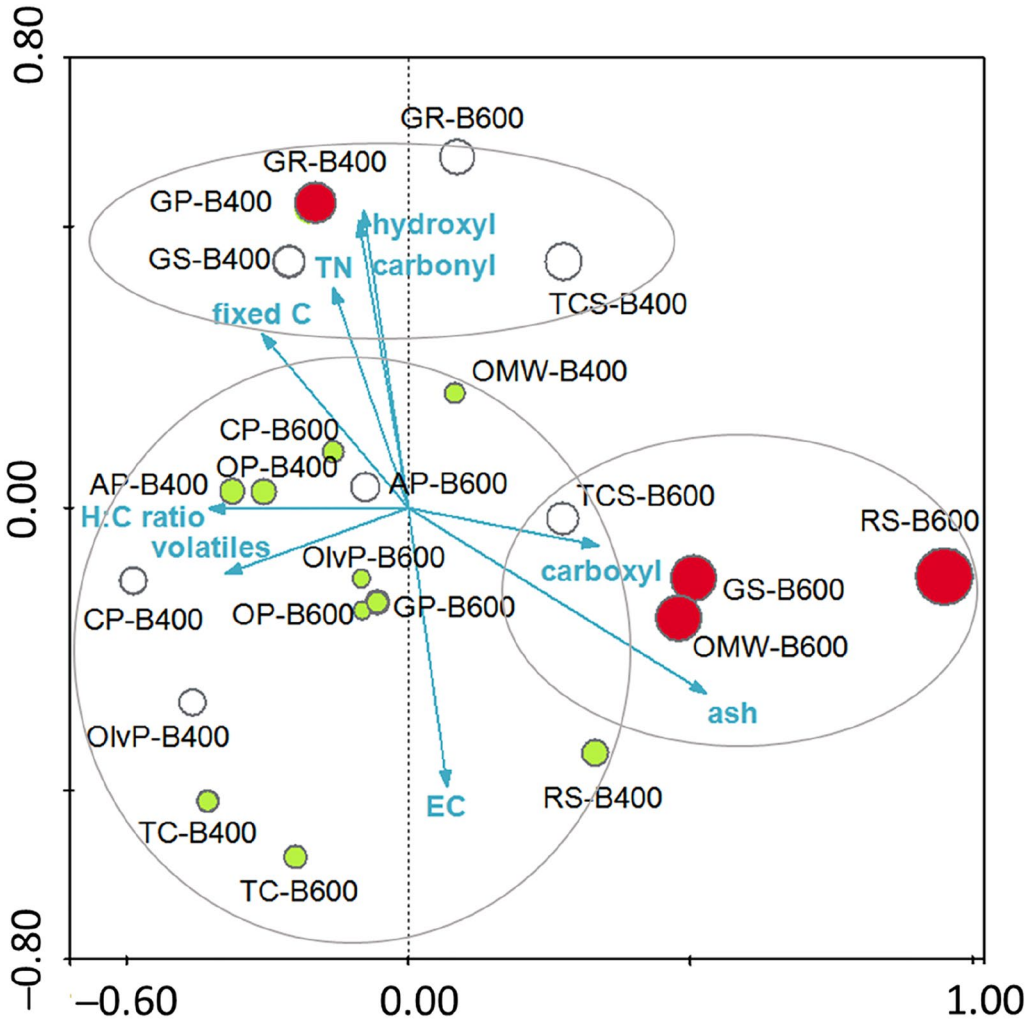

Fig. 4 Redundancy analysis (RDA) correlation biplot showing the relationships between the main physico-chemical characteristics (predictor variables) of the 22 BCs and the cumulative N_2O emissions after BC amendment in experiment 1. The size of the BC symbols corresponds with the quantity of N_2O emitted. Different colours show significant differences between the treatments and control according to the post hoc Dunnet test ($P \leq 0.05$): *green* significant decrease, *red* significant increase, *white* not significantly different to the control. *Blue arrows* point at highest values of BCs properties. H:C ratio represents the atomic ratio of H to organic C, *TN* total N, *carboxyl* carbonyl and hydroxyl represent the percentage of carboxyl, carbonyl and hydroxyl functional groups in BCs surface measured by XPS. EC represents electrical conductivity; ashes, volatiles and fixed C were determined by proximate analysis. Eigenvalues of the first two axes were 0.330 and 0.040, the sum of all canonical axes was 0.371 ($P = 0.001$). *OlvP* olive tree pruning; *OP* orange tree pruning; *GP* grapevine pruning; *CP* carob tree pruning (CP); *GR* giant reed; *RS* rice straw; *TC* tomato crop; *TC+S* tomato crop with substrate; *GS* grape stalks and *OMW* two-phase olive mill waste. B400 and B600 indicate the highest temperature of pyrolysis: 400 and 600 °C, respectively

that decrease N_2O emissions, located in the lower-left quadrant of the figure; (ii) BCs produced at 600 °C that enhance N_2O emissions, positioned on the right side of the figure and (iii) BCs generated at 400 °C that tend to increase N_2O emissions, though their effect is mostly not statistically significant (upper part of the figure). For BCs produced at 400 °C increased N_2O emissions correlated with high N concentrations in BC and higher hydroxyl/quinone functional groups. For BCs produced at 600 °C, increased N_2O emissions correlated with higher carboxylic groups on BCs surface.

In the second experiment (Figure S7), although the number of BCs tested was lower, the RDA confirmed carboxyl functional groups on BC surface as the most important predictor determining increased N_2O emissions after BC soil amendment. The H:Corg molar ratio showed a correlation with N_2 losses in this soil, where N_2 was the primary denitrification product. Biochar physical properties such as TporeA or bulk density did not correlate with neither N_2 nor N_2O emissions. High pH and electrical conductivity were determinants increasing the accumulation of NO_2^- in soil. The concentration of PAHs inversely correlated with N_2 emissions, although the effect was marginal.

4 Discussion

4.1 Denitrification products in the selected soil

In the first experiment, we could not differentiate N_2O produced by denitrification from other pathways. Nonetheless, the experiment enabled us to identify and select BCs with contrasting effects on N_2O emissions under denitrification conditions and pointed at carboxyl groups in BCs produced at 600 °C as an important predictor for high N_2O emissions. In the second experiment, by using the ^{15}N gas-flux method, we could follow the dynamics of N_2O and N_2 primarily produced by denitrification. In this incubation, analyzed ^{15}N data did not reveal any indications that would suggest other potential mechanisms of N gas formation as relevant contributors under the given experimental conditions, such as nitrification, nitrifier-denitrification (Micucci et al. 2023) or co-denitrification (Spott and Stange 2011). Findings from the initial and subsequent incubations largely concur on the impact of biochar on N_2O emissions, with RS-B600 and GS-B600 identified as the BCs that amplified emissions the most.

The selected calcareous soil had a very low denitrification ratio (~0.1), and it could be classified as a "concurrent denitrification" phenotype according to Highton et al. (2022). This implies that N_2O production and reduction steps are synchronized leading to low transitory accumulation of N_2O and thus, low N_2O emissions. This is common in alkaline soils, where the last step of denitrification is usually favored and the main denitrification product is N_2 (Šimek et al. 2002). This phenotype is also favored in fine-textured soils, like in our case, where reduced gas diffusivity promotes N_2O reduction (Gu et al. 2013). Considering that we added a high concentration of NO_3^-, we anticipated that C availability might be a relevant factor constraining denitrification in this soil (Myrold 2021).

4.2 Interaction of BCs with the denitrification process

In this study we demonstrate that BCs interact with the denitrification process and affect denitrification products through several mechanisms, whose prevalence largely depends on BC properties. Biochars with a high H:Corg ratio (>0.5), typical of low temperature of pyrolysis, highly correlated with increased N_2 emissions in soil (Figure S7). This might be a direct consequence of increased C availability to denitrifiers after BCs amendment. C limitation is very likely in soils with large NO_3^- pools, as in our case, and it is known that decreasing the temperature of pyrolysis during BC production increases the fraction of BC decomposable organic C (Wang et al. 2016). This is also supported by our CO_2 data (Figure S8). In general, respiration rates were higher for 400 °C BCs in comparison to their respective 600 °C BCs.

We observed an overall increase in total denitrification with low temperature BCs, although it did not reach statistical significance, likely due to the dispersion of our data. Nevertheless, no corresponding escalation in N_2O emissions was observed, which was linked to a simultaneous reduction of the denitrification ratio by more than 50 percent (i.e. $N_2O/(N_2O+N_2) < 0.05$, with the exception of TC-B400). Thus, selected low temperature BCs showed a tendency to improve soil conditions for denitrification, also promoting a complete reduction of nitrate up to N_2. These results are in good agreement with earlier studies that demonstrated the ability of BC to promote the last step of denitrification (Cayuela et al. 2013; Harter et al. 2014; Weldon et al. 2019).

One of the best characterized factors known to control denitrification and the accumulation of denitrification intermediates is soil pH (Šimek et al. 2002; Frostegård et al. 2022). Previous studies have verified the importance of increased soil pH after BC amendment for the change in stoichiometry of denitrification products in acidic soils (Obia et al. 2015). Nonetheless, considering the high pH and buffering capacity of our soil, a pH effect is very unlikely to act as a relevant driver of observed shifts in N_2O and N_2 production. We postulate that the selected low temperature BCs may directly act as electron donors, facilitating N_2O reduction even under high NO_3^- concentrations. The ability of BC to directly donate electrons to the denitrifying bacteria *P. denitrificans* was recently demonstrated, and BCs with high H:Corg ratio were

found to have a higher reduction index (i.e. the electron donating capacity/electron accepting capacity), which correlated with their ability to promote the reduction of N_2O to N_2 (Pascual et al. 2020). Nevertheless, we cannot discard abiotic redox reactions between N_2O and BCs surface yielding N_2 (Quin et al. 2015).

A second mechanism of interaction consisted in the ability of BCs produced at high temperature (600 °C) to significantly decrease total denitrification losses (N_2+N_2O). The effect of BCs on total denitrification has been much less investigated than its effect on N_2O emissions. Cayuela et al. (2013) found that a BC produced at 500 °C decreased overall denitrification in 10 out of 15 soils. There are several factors that could potentially limit total denitrification, including:

(i) microbial toxicity, i.e. a decline of denitrifiers in soil after BC amendment. Yet, we discard any toxicity effect of BCs produced at 600 °C (except for TC-B600, which is discussed separately below). BCs did not show any signs of toxicity due to high salinity, extreme pH, toxic metals (Sánchez-García et al. 2019) or high concentrations of PAHs (Table S2);

(ii) decreased NO_3^- availability in soil after BC amendment. Several studies have pointed at a decrease in NO_3^- concentrations in soil after BC amendment (Borchard et al. 2019; Martí et al. 2021). Nonetheless, our data on NO_3^- dynamics (Fig. 3) refute this hypothesis, since amendment with high temperature BCs did not decrease NO_3^- concentration in soil compared to the control soil or BCs produced at 400 °C;

(iii) decreased C availability. Although we did not follow DOC dynamics in soil, this could be a plausible explanation for our findings. Biochars produced at high temperatures are known to exert a strong sorptive protection of DOC in soil, which has been related to negative priming (DeCiucies et al. 2018). A decrease in DOC concentration in the soil solution could decrease the DOC/NO_3^- ratios and also inhibit the last step of denitrification, increasing N_2O/(N_2+N_2O) ratios. However, DOC has been found to minimally affect the product ratio of denitrification in soils with high NO_3^- concentrations, as in our case (Senbayram et al. 2012). Further investigation is warranted, particularly involving varied initial NO_3^- additions to the soil;

(iv) increased oxygen concentration in soil. Oxygen affects denitrification by regulating enzyme synthesis and in particular by inhibiting enzyme activity (Myrold 2021). BCs might have increased soil aeration in our heavy textured soil, which could explain both lower denitrification and higher N_2O/(N_2+N_2O) ratios. However, we found no relationship between the physical properties of BCs (total pore area and bulk density) and denitrification products (Figure S7). In fact the physical properties of BCs were governed by feedstock rather than by the temperature of pyrolysis (Sánchez-García et al. 2019), whereas the effect of BC on total denitrification was dependent on the temperature of pyrolysis.

(v) the presence of quinone moieties in high temperature BCs has been related to lower denitrification rates because of their ability to compete with NO_3^- as electron acceptors (Chen et al. 2018). In addition, quinone moieties were occasionally reported to interact also with other microbial N turnover processes like urea hydrolysis and nitrification (Xu et al. 2000; Papadopoulou et al. 2022). This mechanism might also account for the increased N_2O/(N_2O+N_2) ratios with high temperature BCs, as carbonyl groups could similarly compete with N_2O for electrons. Although we did not find any direct relationship between carbonyl groups in BCs and total denitrification, this mechanism deserves further investigation.

Whereas it has been generally assumed that the key mechanism of BC to decrease N_2O emissions is the promotion of the last step of denitrification (N_2O transformation to N_2), here we show that, in alkaline soils, this mechanism might be primarily relevant for low temperature BCs. Nevertheless, recent meta-analyses indicate that BCs produced at high temperatures (H:Corg ratio < 0.3) offer the greatest potential for N_2O mitigation, which seems in contradiction with our findings. Our study shows that BCs produced at 600 °C might operate through a different mechanism, i.e. decreasing total denitrification. In our soil, lower denitrification was not translated to lower N_2O emissions because of the change in stoichiometry of denitrification products. Further studies are required to understand the mechanisms behind this trade-off. As discussed previously, it might be related to changes in DOC/NO_3^- ratios or to the presence of oxygenated groups in BCs surface, which might compete with both NO_3^- and N_2O as electron acceptors. In this study we found that a high concentration of carboxyl groups in our 600 °C BCs surface was highly correlated with higher N_2O emissions. Nevertheless, it is important to note that the presence of carboxyl groups is associated with the original feedstock and post-pyrolysis treatments rather than the temperature of pyrolysis.

Biochars produced from tomato crops represented a clear exception. Even if their general properties might potentially allow similar effects on denitrification as observed for the other selected BCs, their application was

accompanied by a significant negative impact on microbial activity in general as seen by the low CO_2 respiration rate, in particular concerning TC-B600.

These BCs displayed phytotoxicity, with germination indices <30% (Pascual 2021), a very high EC (18–23 mS cm^{-1}) and TC-B600 also exhibited an extremely high pH (12.2). The response of denitrifiers to high EC is similar to that of other soil heterotrophs, which usually decrease their activity (Adviento-Borbe et al. 2006; Setia et al. 2010). Indeed, we observed that TC-B600 minimized total denitrification (Fig. 2) and basically ceased soil respiration (Figure S8), which can be considered a strong indicator of toxicity. The negative CO_2 fluxes may be attributed to the high pH of this BC, which can induce CO_2 capture in soil and the formation of secondary carbonates, a phenomenon previously observed in other calcareous soils after BC amendment (Wang et al. 2023).

Amendment with TC-B600 also modified the dynamics of NO_3^- and NO_2^- in soil, being the only treatment with high NO_2^- concentrations throughout the entire incubation. Although, to some degree, all treatments exhibited nitrite accumulation, the NO_2^-/NO_3^- ratios in TC treatments were the highest. Nitrite may well accumulate in soil under denitrifying conditions and high pH values and this is indicative of a soil where the activity of nitrate reductase (NAR) is favored in comparison to nitrite reductase (NIR) (Lim et al. 2018). The high concentration of NO_2^- in these treatments suggests that chemodenitrification might be partially responsible for N_2O emissions (Zhu-Barker et al. 2015).

We postulate that the NO_2^- accumulation in TC-B600 treatment can be attributed to the inhibition of NIR activity in soil due to the environmental stress induced by this BC. Nitrate reductase is generally regarded as more resilient and better able to withstand environmental stress compared to NIR which has been found to be more sensitive to changes in pH and salinity (Yoshie et al. 2004; Albina et al. 2019).

4.3 Characteristics of BCs that might increase N_2O emissions

Nitrogen content and pH in BCs are well-known factors modulating denitrification. Nitrogen-rich BCs serve as a substrate for nitrification, which will ultimately lead to denitrification and increased N_2O emissions. Additionally, the alkaline properties of BC are recognized to play a significant role in facilitating the last step of denitrification and reducing N_2O emissions in acid soils (Obia et al. 2015). Ruling these two factors out, both RDA analyses pointed at carboxyl groups in BC surface as the main predictor for increased N_2O emissions. This is in accordance with previous findings by Yuan et al. (2019), who demonstrated that a BC that was chemically oxydized with H_2O_2 missed its N_2O mitigation potential. Later, the same authors showed that carboxyl-loaded graphene significantly decreased the genetic potential for N_2O reduction and increased the $N_2O/(N_2O+N_2)$ ratio in soil slurries (Yuan et al. 2021). The reasons behind these findings are probably related to the lower electron donating capacity of these BCs, since the carboxyl group is the most oxidized of all oxygen containing functional groups and considered to be redox inactive. This is known to limit the transport of electrons through the aromatic structure of BCs (Chacón et al. 2020).

In general, the number of oxygen-containing functional groups on BCs surface decreases with pyrolysis temperature (Chacón et al. 2020). On the contrary, carboxyl groups do not necessarily follow the same pattern, and their concentration is heavily influenced by the specific feedstock used (Chen et al. 2015; Chacón et al. 2020). From our 22 selected BCs, those produced from tomato crops and olive mill wastes registered the highest concentration of carboxyl moieties (at both 400 and 600 °C), whereas grape stalks registered high values only at 600 °C (Table S1). Understanding which feedstocks and pyrolysis conditions yield BCs with high concentrations of carboxyl moieties seems therefore essential for making informed decisions and selecting appropriate BCs for N_2O mitigation.

We hypothesized that the concentration of PAHs in BC might be correlated with higher N_2O emissions, as previous studies found (Alburquerque et al. 2015). In our study, even though a weak association between PAHs concentration and N_2O emissions was found (Figure S7), our results seem to indicate that the PAHs at the low concentrations found in our selected BCs (between 31 and 177 μg C kg^{-1} soil) did not represent a risk and did not play a major role in modulating N_2O emissions.

Finally, DOC was not a good predictor of C availability in BCs. Its value was generally low for all BCs (1–8 g kg^{-1} soil) and depended on the original feedstock more than the pyrolysis temperature. While the correlation between dissolved organic carbon (DOC) in organic amendments and denitrification activity has been observed in previous studies (Surey et al. 2020), for BCs the H:Corg was a more effective indicator for C accessibility.

5 Conclusions and future research needs

Multivariate analysis showed that a high concentration of carboxyl groups in BCs surface was highly correlated with increased N_2O emissions after BC amendment, whereas DOC, PAHs and physical properties such as pore area and bulk density did not seem to be relevant modulating total denitrification or the stoichiometry of denitrification products. High electrical conductivity and pH in BCs were related to increased NO_2^-/NO_3^- ratios

in soil, although this effect was accompained by a overall decrease in microbial activity and did not imply higher N_2O emissions.

Our study clearly illustrates that BC interacts with denitrification in varying ways depending on the BC characteristics. Ideally, BCs should decrease both total denitrification (to enhance crop N use efficiency) and the denitrification ratio (to mitigate harmful N_2O emissions). Our findings reveal that BCs produced at 600 °C significantly reduced total N loss by denitrification (N_2+N_2O), but there was a trade-off with the denitrification ratios, which seems to be linked to carboxyl groups on BCs surface. As our ^{15}N experiment lacked a sufficient number of high-temperature BCs with a low concentration of carboxyl groups, we were unable to demonstrate the feasibility of reducing N loss while maintaining or even decreasing denitrification ratios. Further studies are necessary, including a wide array of high-temperature BCs with varying concentrations of carboxyl groups to address this dilemma.

In addition, it remains challenging why N losses due to denitrification (N_2O+N_2) decrease significantly with BCs produced at 600 °C. This is especially puzzling given that soil NO_3^- concentrations remained consistent across both high and low-temperature BCs, and NO_3^- consumption was similar by the end of the incubation. Further research is needed to determine the whereabouts of this nitrogen discrepancy—whether it is retained in soil as organic N or lost as gases other than N_2O and N_2.

Supplementary Information

The online version contains supplementary material available at https://doi.org/10.1007/s42773-024-00386-3.

Additional file 1.

Acknowledgements
This work was supported by the Project PID2021-128896OB-I00 funded by MCIN/AEI/https://doi.org/10.13039/501100011033/ and ERDF A way of making Europe. Additional funds were provided by the project Nº 201840I127 from CSIC.

Author contributions
MLC, MASM, MBP and MSG contributed to the study conception and design. MBP and MSG carried out the experiments. MLC and OS analyzed the data. MLC wrote the initial draft and all authors contributed to writing in different sections of the manuscript. All authors read and approved the final manuscript. MASM and MLC secured the funding.

Funding
Open Access funding provided thanks to the CRUE-CSIC agreement with Springer Nature. Public competitive calls PID2021-128896OB-I00 funded by MCIN/AEI/https://doi.org/10.13039/501100011033/ and ERDF A way of making Europe and project Nº 201840I127 from CSIC.

Declarations

Ethics approval and consent to participate
This manuscript does not report on or involve any animals, humans, human data, human tissue or plants, so this section is not applicable.

Consent for publication
Not applicable.

Availability of data and materials
Raw data used to produce figures will be made available on reasonable request.

Competing interests
The authors declare that they have no known competing financial interests or personal relationships that could have influenced the work reported in this paper.

Author details
[1]Department of Soil and Water Conservation and Waste Management, CEBAS-CSIC. Campus Universitario de Espinardo, 30100 Murcia, Spain. [2]SKW Stickstoffwerke Piesteritz GmbH. Agricultural Application Research, 04451 Borsdorf, Germany.

Received: 18 June 2024 Revised: 5 September 2024 Accepted: 9 September 2024
Published online: 21 October 2024

References

Adviento-Borbe MAA, Doran JW, Drijber RA, Dobermann A (2006) Soil electrical conductivity and water content affect nitrous oxide and carbon dioxide emissions in intensively managed soils. J Environ Qual 35:1999–2010. https://doi.org/10.2134/jeq2006.0109

Albina P, Durban N, Bertron A, Albrecht A, Robinet J-C, Erable B (2019) Influence of hydrogen electron donor, alkaline pH, and high nitrate concentrations on microbial denitrification: a review. Int J Mol Sci 20(20):5163. https://doi.org/10.3390/ijms20205163

Alburquerque JA, Sánchez-Monedero MA, Roig A, Cayuela ML (2015) High concentrations of polycyclic aromatic hydrocarbons (naphthalene, phenanthrene and pyrene) failed to explain biochar's capacity to reduce soil nitrous oxide emissions. Environ Pollut 196:72–77. https://doi.org/10.1016/j.envpol.2014.09.014

Berendt J, Tenspolde A, Rex D, Clough TJ, Wrage-Mönnig N (2020) Application methods of tracers for N_2O source determination lead to inhomogeneous distribution in field plots. Anal Sci Adv 1:221–232. https://doi.org/10.1002/ansa.202000100

Borchard N, Schirrmann M, Cayuela ML, Kammann C, Wrage-Mönnig N, Estavillo JM, Fuertes-Mendizábal T, Sigua G, Spokas K, Ippolito JA, Novak J (2019) Biochar, soil and land-use interactions that reduce nitrate leaching and N_2O emissions: a meta-analysis. Sci Total Environ 651:2354–2364. https://doi.org/10.1016/j.scitotenv.2018.10.060

Cayuela ML, Jeffery S, van Zwieten L (2015) The molar H: Corg ratio of biochar is a key factor in mitigating N_2O emissions from soil. Agric Ecosyst Environ 202:135–138. https://doi.org/10.1016/j.agee.2014.12.015

Cayuela ML, Oenema O, Kuikman PJ, Bakker RR, Van Groenigen JW (2010) Bioenergy by-products as soil amendments? Implications for carbon sequestration and greenhouse gas emissions. GCB Bioenergy 2:201–213. https://doi.org/10.1111/j.1757-1707.2010.01055.x

Cayuela ML, Sánchez-Monedero MA, Roig A, Hanley K, Enders A, Lehmann J (2013) Biochar and denitrification in soils: when, how much and why does biochar reduce N_2O emissions? Sci Rep 3:1732. https://doi.org/10.1038/srep01732

Cayuela ML, van Zwieten L, Singh BP, Jeffery S, Roig A, Sánchez-Monedero MA (2014) Biochar's role in mitigating soil nitrous oxide emissions: a review and meta-analysis. Agr Ecosyst Environ 191:5–16. https://doi.org/10.1016/j.agee.2013.10.009

Chacón FJ, Sánchez-Monedero MA, Lezama L, Cayuela ML (2020) Enhancing biochar redox properties through feedstock selection, metal preloading and post-pyrolysis treatments. Chem Eng J 395:12100

Chen Z, Xiao X, Chen B, Zhu L (2015) Quantification of chemical states, dissociation constants and contents of oxygen-containing groups on the surface of biochars produced at different temperatures. Environ Sci Technol 49:309–317. https://doi.org/10.1021/es5043468

Chen G, Zhang Z, Zhang Z, Zhang R (2018) Redox-active reactions in denitrification provided by biochars pyrolyzed at different temperatures. Sci Total Environ 615:1547–1556. https://doi.org/10.1016/j.scitotenv.2017.09.125

DeCiucies S, Whitman T, Woolf D, Enders A, Lehmann J (2018) Priming mechanisms with additions of pyrogenic organic matter to soil. Geochim Cosmochim Acta 238:329–342. https://doi.org/10.1016/j.gca.2018.07.004

Dong W, Walkiewicz A, Bieganowski A, Oenema O, Nosalewicz M, He C, Zhang Y, Hu C (2020) Biochar promotes the reduction of N_2O to N_2 and concurrently suppresses the production of N_2O in calcareous soil. Geoderma 362:114091. https://doi.org/10.1016/j.geoderma.2019.114091

Fan C, Duan P, Zhang X, Shen H, Chen M, Xiong Z (2020) Mechanisms underlying the mitigation of both N_2O and NO emissions with field-aged biochar in an Anthrosol. Geoderma 364:114178. https://doi.org/10.1016/j.geoderma.2020.114178

Frostegård Å, Vick SHW, Lim NYN, Bakken LR, Shapleigh JP (2022) Linking meta-omics to the kinetics of denitrification intermediates reveals pH-dependent causes of N_2O emissions and nitrite accumulation in soil. ISME J 16:26–37. https://doi.org/10.1038/s41396-021-01045-2

Grados D, Butterbach-Bahl K, Chen J, Jan van Groenigen K, Olesen JE, Willem van Groenigen J, Abalos D (2022) Synthesizing the evidence of nitrous oxide mitigation practices in agroecosystems. Environ Res Lett 17:114024. https://doi.org/10.1088/1748-9326/ac9b50

Gu J, Nicoullaud B, Rochette P, Grossel A, Hénault C, Cellier P, Richard G (2013) A regional experiment suggests that soil texture is a major control of N_2O emissions from tile-drained winter wheat fields during the fertilization period. Soil Biol Biochem 60:134–141. https://doi.org/10.1016/j.soilbio.2013.01.029

Harter J, Krause H-M, Schuettler S, Ruser R, Fromme M, Scholten T, Kappler A, Behrens S (2014) Linking N_2O emissions from biochar-amended soil to the structure and function of the N-cycling microbial community. ISME J 8:660–674. https://doi.org/10.1038/ismej.2013.160

Harvey MJ, Sperlich P, Clough TJ, Kelliher FM, McGeough KL, Martin RJ, Moss R (2020) Global Research Alliance N_2O chamber methodology guidelines: recommendations for air sample collection, storage, and analysis. J Environ Qual 49:1110–1125. https://doi.org/10.1002/jeq2.20129

Highton MP, Bakken LR, Dörsch P, Molstad L, Morales SE (2022) Nitrite accumulation and impairment of N_2O reduction explains contrasting soil denitrification phenotypes. Soil Biol Biochem 166:108529. https://doi.org/10.1016/j.soilbio.2021.108529

Hilber I, Blum F, Leifeld J, Schmidt H-P, Bucheli TD (2012) Quantitative determination of PAHs in biochar: a prerequisite to ensure its quality and safe application. J Agric Food Chem 60:3042–3050. https://doi.org/10.1021/jf205278v

Joseph S, Cowie AL, Van Zwieten L, Bolan N, Budai A, Buss W, Cayuela ML, Graber ER, Ippolito JA, Kuzyakov Y, Luo Y, Ok YS, Palansooriya KN, Shepherd J, Stephens S, Weng (Han) Z, Lehmann J (2021) How biochar works, and when it doesn't: a review of mechanisms controlling soil and plant responses to biochar. GCB Bioenergy 13:1731–1764. https://doi.org/10.1111/gcbb.12885

Kaur N, Kieffer C, Ren W, Hui D (2023) How much is soil nitrous oxide emission reduced with biochar application? An evaluation of meta-analyses. GCB Bioenergy 15:24–37. https://doi.org/10.1111/gcbb.13003

Lehmann J, Cowie A, Masiello CA, Kammann C, Woolf D, Amonette JE, Cayuela ML, Camps-Arbestain M, Whitman T (2021) Biochar in climate change mitigation. Nat Geosci 14:883–892. https://doi.org/10.1038/s41561-021-00852-8

Lim NYN, Frostegård Å, Bakken LR (2018) Nitrite kinetics during anoxia: the role of abiotic reactions versus microbial reduction. Soil Biol Biochem 119:203–209. https://doi.org/10.1016/j.soilbio.2018.01.006

Liu Q, Liu B, Zhang Y, Hu T, Lin Z, Liu G, Wang X, Ma J, Wang H, Jin H, Ambus P, Amonette JE, Xie Z (2019) Biochar application as a tool to decrease soil nitrogen losses (NH_3 volatilization, N_2O emissions, and N leaching) from croplands: options and mitigation strength in a global perspective. Glob Change Biol 25:2077–2093. https://doi.org/10.1111/gcb.14613

Maenhout P, Di Bene C, Cayuela ML, Diaz-Pines E, Govednik A, Keuper F, Mavsar S, Mihelic R, O'Toole A, Schwarzmann A, Suhadolc M, Syp A, Valkama E (2024) Trade-offs and synergies of soil carbon sequestration: addressing knowledge gaps related to soil management strategies. Eur J Soil Sci 75:e13515. https://doi.org/10.1111/ejss.13515

Martí E, Sierra J, Domene X, Mumbrú M, Cruañas R, Garau MA (2021) One-year monitoring of nitrogen forms after the application of various types of biochar on different soils. Geoderma 402:115178. https://doi.org/10.1016/j.geoderma.2021.115178

Micucci G, Sgouridis F, McNamara NP, Krause S, Lynch I, Roos F, Well R, Ullah S (2023) The ^{15}N-Gas flux method for quantifying denitrification in soil: current progress and future directions. Soil Biol Biochem 9:109–108. https://doi.org/10.1016/j.soilbio.2023.109108

Miller JC, Miller JN (1992) Statistics for analytical chemistry, 2nd edn. Prentice Hall, Englewood Cliffs

Myrold DD (2021) 15-Transformations of nitrogen. In: Gentry TJ, Fuhrmann JJ, Zuberer DA (eds), Principles and applications of soil microbiology, 3rd edition, pp 385–421. Elsevier, Amsterdam. https://doi.org/10.1016/B978-0-12-820202-9.00015-0

Obia A, Cornelissen G, Mulder J, Dörsch P (2015) Effect of soil pH increase by biochar on NO, N_2O and N_2 production during denitrification in acid soils. PLoS ONE 10:e0138781. https://doi.org/10.1371/journal.pone.0138781

Ogle SM, Butterbach-Bahl K, Cardenas L, Skiba U, Scheer C (2020) From research to policy: optimizing the design of a national monitoring system to mitigate soil nitrous oxide emissions. Curr Opin Env Sust 47:28–36. https://doi.org/10.1016/j.cosust.2020.06.003

Papadopoulou ES, Bachtsevani CL, Papazlatani CV, Rousidou C, Brouziotis A, Lampronikou E, Tsiknia M, Vasileiadis S, Ipsilantis I, Menkissoglu-Spiroudi U, Ehaliotis C, Philippot L, Nicol GW, Karpouzas DG (2022) The effects of quinone imine, a new potent nitrification inhibitor, dicyandiamide, and nitrapyrin on target and off-target soil microbiota. Microbiol Spectrum 10:e02403-e2421. https://doi.org/10.1128/spectrum.02403-21

Pascual MB (2021) Relevance of biochar properties for the emission of greenhouse gases in agricultural soils, PhD Thesis. Universidad de Murcia, Escuela Internacional de Doctorado.

Pascual MB, Sanchez-Monedero MA, Cayuela ML, Li S, Haderlein SB, Ruser R, Kappler A (2020) Biochar as electron donor for reduction of N_2O by *Paracoccus denitrificans*. FEMS Microbiol Ecol 96(8):fiaa133. https://doi.org/10.1093/femsec/fiaa133

Quin P, Joseph S, Husson O, Donne S, Mitchell D, Munroe P, Phelan D, Cowie A, Van Zwieten L (2015) Lowering N_2O emissions from soils using eucalypt biochar: the importance of redox reactions. Sci Rep 5:16773. https://doi.org/10.1038/srep16773

Sánchez-García M, Cayuela ML, Rasse DP, Sánchez-Monedero MA (2019) Biochars from Mediterranean agroindustry residues: physicochemical properties relevant for C sequestration and soil water retention. ACS Sustain Chem Eng 7:4724–4733. https://doi.org/10.1021/acssuschemeng.8b04589

Sanchez-Garcia M, Roig A, Sánchez-Monedero MA, Cayuela ML (2014) Biochar increases soil N_2O emissions produced by nitrification-mediated pathways. Front Environ Sci. https://doi.org/10.3389/fenvs.2014.00025

Senbayram M, Chen R, Budai A, Bakken L, Dittert K (2012) N_2O emission and the $N_2O/(N_2O+N_2)$ product ratio of denitrification as controlled by available carbon substrates and nitrate concentrations. Mitig Environ Impacts Nitrogen Use Agric 147:4–12. https://doi.org/10.1016/j.agee.2011.06.022

Setia R, Marschner P, Baldock J, Chittleborough D (2010) Is CO_2 evolution in saline soils affected by an osmotic effect and calcium carbonate? Biol Fertil Soils 46:781–792. https://doi.org/10.1007/s00374-010-0479-3

Šimek M, JíšováHopkins LDW (2002) What is the so-called optimum pH for denitrification in soil? Soil Biol Biochem 34:1227–1234. https://doi.org/10.1016/S0038-0717(02)00059-7

Singh B, Camps-Arbestain M, Lehmann J (2017) Biochar. A guide to analytical methods. Chapter 6. Dissolved carbon and LC-OCD of biochar. CRC Press/Taylor and Francis Group LLC

Sommer SG, Kjellerup V, Kristjansen O (1992) Determination of total ammonium nitrogen in pig and cattle slurry: sample preparation and analysis. Acta Agric Scand B 42:146–151. https://doi.org/10.1080/09064719209417969

Spott O, Russow R, Apelt B, Stange CF (2006) A ^{15}N-aided artificial atmosphere gas flow technique for online determination of soil N_2 release using the zeolite Köstrolith SX6®. Rapid Commun Mass Spectrom 20:3267–3274. https://doi.org/10.1002/rcm.2722

Spott O, Stange F (2011) Formation of hybrid N_2O in a suspended soil due to co-denitrification of NH_2OH. J Plant Nutr Soil Sci 174:554–567. https://doi.org/10.1002/jpln.201000200

Surey R, Schimpf CM, Sauheitl L, Mueller CW, Rummel PS, Dittert K, Kaiser K, Böttcher J, Mikutta R (2020) Potential denitrification stimulated by water-soluble organic carbon from plant residues during initial decomposition. Soil Biol Biochem 147:107841. https://doi.org/10.1016/j.soilbio.2020.107841

Ter Brak JCF, Smilauer P (1998) Canoco reference manual and user's guide to Canoco for windows: software for canonical community ordination (version 4). Microcomputer Power, Ithaca, NY, USA

Thomazini A, Spokas K, Hall K, Ippolito J, Lentz R, Novak J (2015) GHG impacts of biochar: predictability for the same biochar. Agr Ecosyst Environ 207:183–191. https://doi.org/10.1016/j.agee.2015.04.012

Thompson RL, Lassaletta L, Patra PK, Wilson C, Wells KC, Gressent A, Koffi EN, Chipperfield MP, Winiwarter W, Davidson EA, Tian H, Canadell JG (2019) Acceleration of global N_2O emissions seen from two decades of atmospheric inversion. Nat Clim Chang 9:993–998. https://doi.org/10.1038/s41558-019-0613-7

Tian H, Xu R, Canadell JG, Thompson RL, Winiwarter W, Suntharalingam P, Davidson EA, Ciais P, Jackson RB, Janssens-Maenhout G, Prather MJ, Regnier P, Pan N, Pan S, Peters GP, Shi H, Tubiello FN, Zaehle S, Zhou F, Arneth A, Battaglia G, Berthet S, Bopp L, Bouwman AF, Buitenhuis ET, Chang J, Chipperfield MP, Dangal SRS, Dlugokencky E, Elkins JW, Eyre BD, Fu B, Hall B, Ito A, Joos F, Krummel PB, Landolfi A, Laruelle GG, Lauerwald R, Li W, Lienert S, Maavara T, MacLeod M, Millet DB, Olin S, Patra PK, Prinn RG, Raymond PA, Ruiz DJ, van der Werf GR, Vuichard N, Wang J, Weiss RF, Wells KC, Wilson C, Yang J, Yao Y (2020) A comprehensive quantification of global nitrous oxide sources and sinks. Nature 586:248–256. https://doi.org/10.1038/s41586-020-2780-0

Wang J, Xiong Z, Kuzyakov Y (2016) Biochar stability in soil: meta-analysis of decomposition and priming effects. GCB Bioenergy 8:512–523. https://doi.org/10.1111/gcbb.12266

Wang Y, Joseph S, Wang X, Weng ZH, Mitchell DRG, Nancarrow M, Taherymoosavi S, Munroe P, Li G, Lin Q, Chen Q, Flury M, Cowie A, Husson O, Van Zwieten L, Kuzyakov Y, Lehmann J, Li B, Shang J (2023) Inducing inorganic carbon accrual in subsoil through biochar application on calcareous topsoil. Environ Sci Technol 57:1837–1847. https://doi.org/10.1021/acs.est.2c06419

Weldon S, Rasse DP, Budai A, Tomic O, Dörsch P (2019) The effect of a biochar temperature series on denitrification: which biochar properties matter? Soil Biol Biochem 135:173–183. https://doi.org/10.1016/j.soilbio.2019.04.018

Wickham H (2016) ggplot2: Elegant graphics for data analysis

Winiwarter W, Höglund-Isaksson L, Klimont Z, Schöpp W, Amann M (2018) Technical opportunities to reduce global anthropogenic emissions of nitrous oxide. Environ Res Lett 13:014011. https://doi.org/10.1088/1748-9326/aa9ec9

WRB (2022) IUSS Working Group. World Reference Base for Soil Resources. International soil classification system for naming soils and creating legends for soil maps. 4th edition. International Union of Soil Sciences (IUSS), Vienna, Austria.

Wu Z, Dong Y, Zhang X, Xu X, Xiong Z (2023) Biochar single application and reapplication decreased soil greenhouse gas and nitrogen oxide emissions from rice–wheat rotation: a three-year field observation. Geoderma 435:116498. https://doi.org/10.1016/j.geoderma.2023.116498

Xu X, Zhou L, Van Cleemput O, Wang Z (2000) Fate of urea-^{15}N in a soil-wheat system as influenced by urease inhibitor hydroquinone and nitrification inhibitor dicyandiamide. Plant Soil 220:261–270. https://doi.org/10.1023/A:1004715827085

Yoshie S, Noda N, Tsuneda S, Hirata A, Inamori Y (2004) Salinity decreases nitrite reductase gene diversity in denitrifying bacteria of wastewater treatment systems. Appl Environ Microbiol 70:3152–3157. https://doi.org/10.1128/AEM.70.5.3152-3157.2004

Yuan D, Yuan H, He X, Hu H, Qin S, Clough T, Wrage-Mönnig N, Luo J, He X, Chen M, Zhou S (2021) Identification and verification of key functional groups of biochar influencing soil N_2O emission. Biol Fertil Soils 57:447–456. https://doi.org/10.1007/s00374-021-01541-9

Yuan H, Zhang Z, Li M, Clough T, Wrage-Mönnig N, Qin S, Ge T, Liao H, Zhou S (2019) Biochar's role as an electron shuttle for mediating soil N_2O emissions. Soil Biol Biochem 133:94–96. https://doi.org/10.1016/j.soilbio.2019.03.002

Zhu-Barker X, Cavazos AR, Ostrom NE, Horwath WR, Glass JB (2015) The importance of abiotic reactions for nitrous oxide production. Biogeochemistry 126:251–267. https://doi.org/10.1007/s10533-015-0166-4

Zhu-Barker X, Steenwerth KL (2018) Chapter Six - Nitrous oxide production from soils in the future: processes, controls, and responses to climate change, In: Horwath WR, Kuzyakov Y (eds), Developments in soil science, pp 131–183. Elsevier, Amsterdam. https://doi.org/10.1016/B978-0-444-63865-6.00006-5